Supporting Information

Highly Conjugated 2D COF/MOF Composites for Bifunctional Electrocatalytic Alkaline HER and OER with enhanced activity and stability

Yang Liu,[a,b] Zhao-Di Yang,*[a] Rui Zhang,[a] Yingchao Lai,[a] Yu Zhang*[b] and Guiling Zhang[a]

[a.] *Heilongjiang Provincial Key Laboratory of CO_2 Resource Utilization and Energy Catalytic Materials, School of Materials Science and Chemical Engineering, Harbin University of Science and Technology, Harbin, Heilongjiang, 150080, PR China.*

[b.] *Institute of Process Engineering, Chinese Academy of Sciences, Beijing, 100080, Beijing, PR China.*

*Corresponding authors

E-mail: yangzhaodi@163.com (Z.-D. Yang); zhangyu@ipe.ac.cn (Y. Zhang)

Supplementary Figures

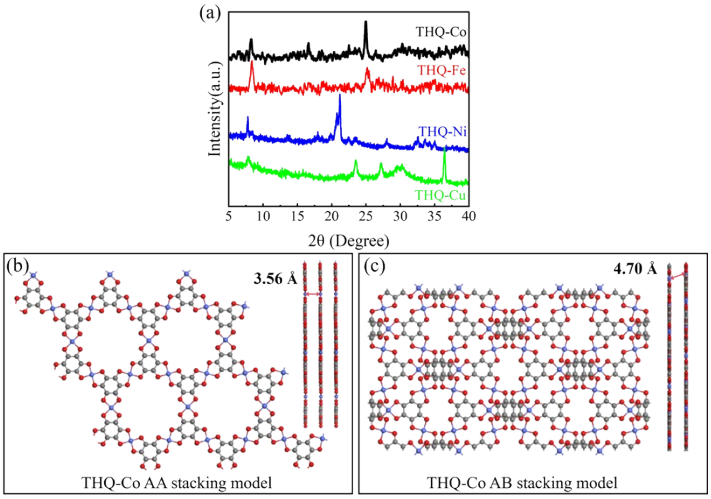

Fig. S1 (a) XRD pattern of THQ-M samples, (b) AA and (c) AB stacking models of THQ-Co.

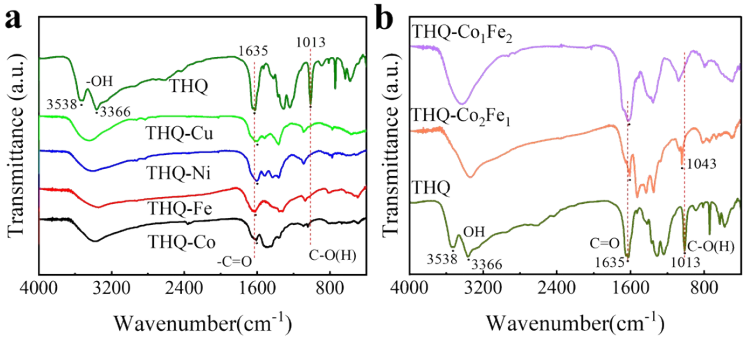

Fig. S2 Infrared spectra of THQ-M samples.

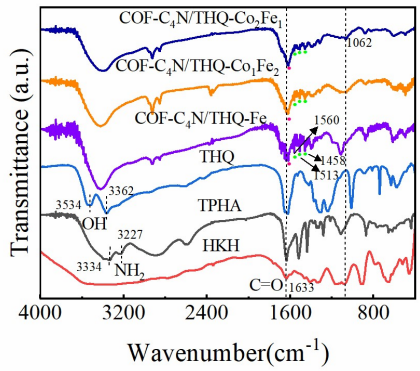

Fig. S3 IR spectra of COF-C_4N/THQ-Fe, COF-C_4N/THQ-Co_1Fe_2 and COF-C_4N/THQ-Co_2Fe_1 composite catalysts.

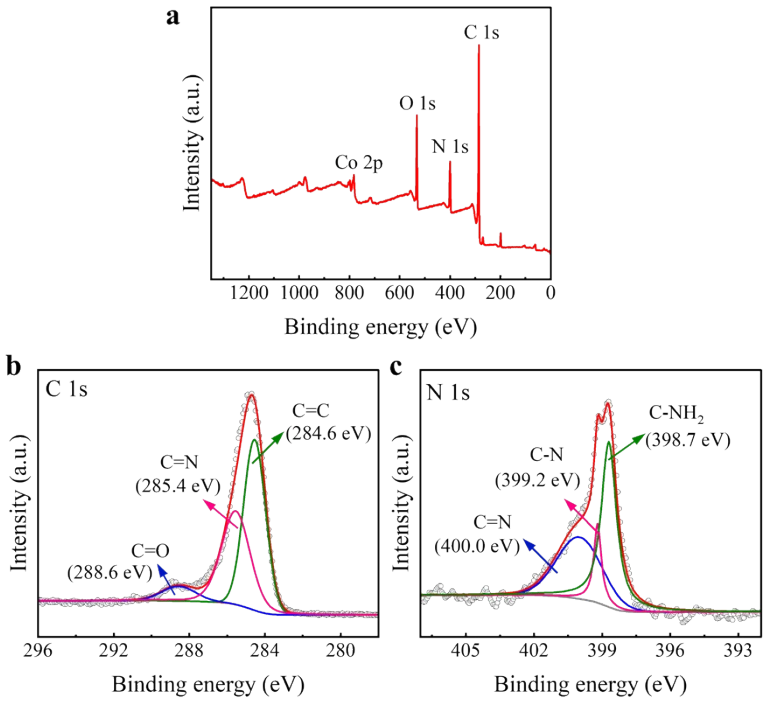

Fig. S4 (a) XPS total spectrum of COF-C_4N/THQ-Co sample. XPS spectra of the COF-C_4N: (b) C 1s and (c) N 1s.

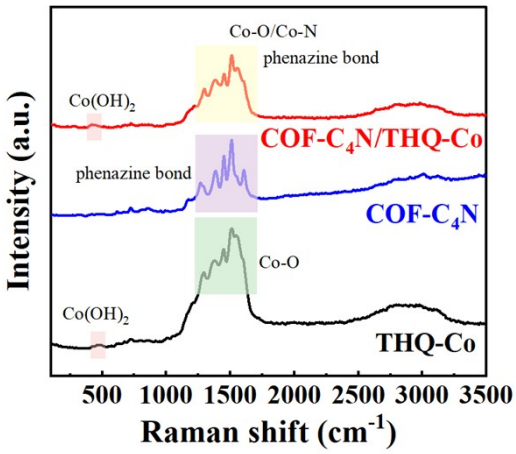

Fig. S5 Raman spectra of THQ-Co, COF-C_4N, and COF-C_4N/THQ-Co.

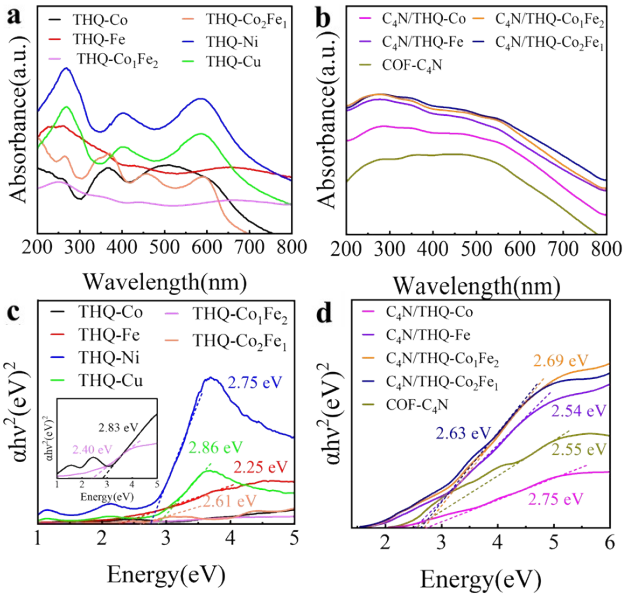

Fig. S6 (a-b) UV-Vis diffuse reflectance spectrum and (c-d) Tauc plot of THQ-M, COF-C_4N/THQ-M and COF-C_4N.

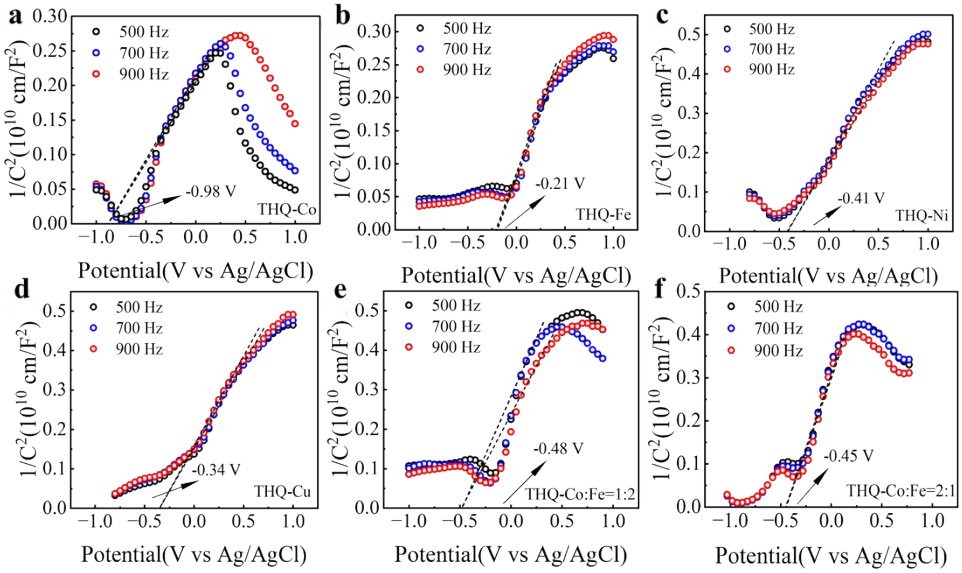

Fig. S7 (a-f) Mott-Schottky plots of THQ-M.

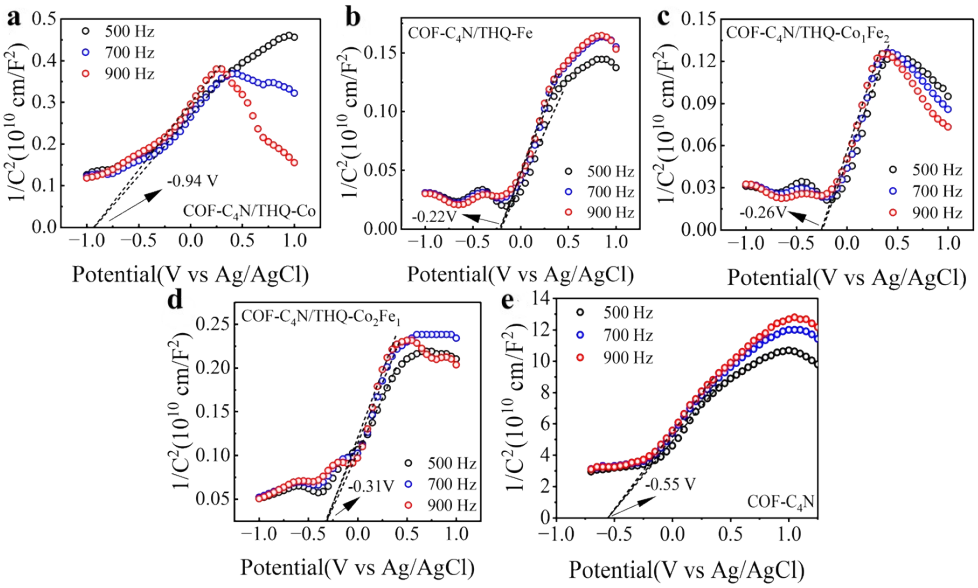

Fig. S8 Mott-Schottky plots of (a-d) COF-C_4N/THQ-M and (e) COF-C_4N.

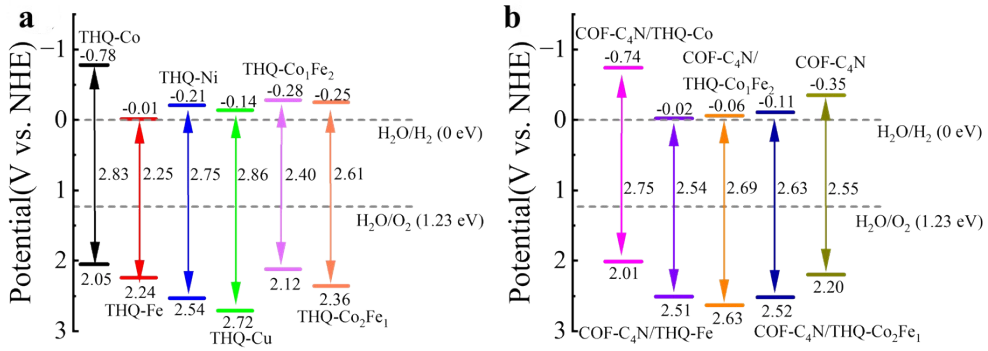

Fig. S9 Diagrams of the energy level of the valence and conduction band for (a) THQ-M and (b) COF-C_4N /THQ-M and COF-C_4N.

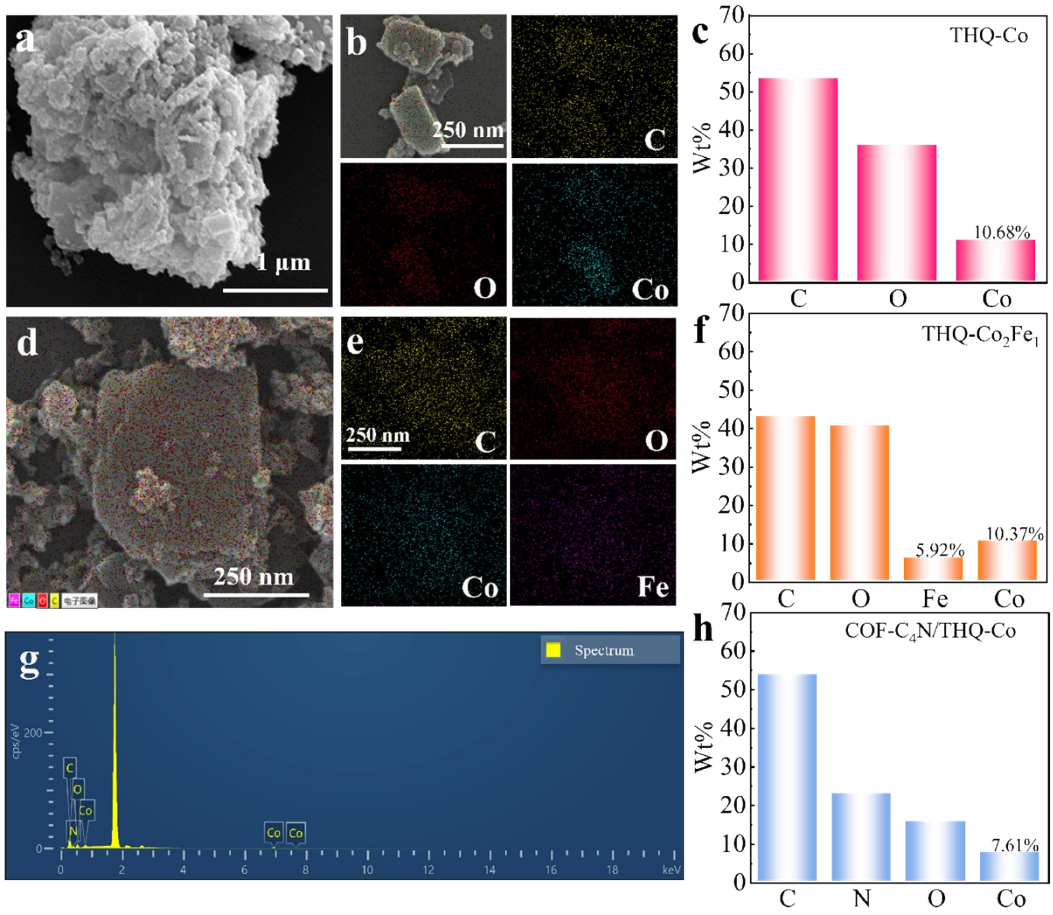

Fig. S10 Sample THQ-Co for (a-c) SEM image, EDS elemental analysis and content of each element. THQ-Co_2Fe_1 for (d-f) EDS elemental analysis and content of each element.

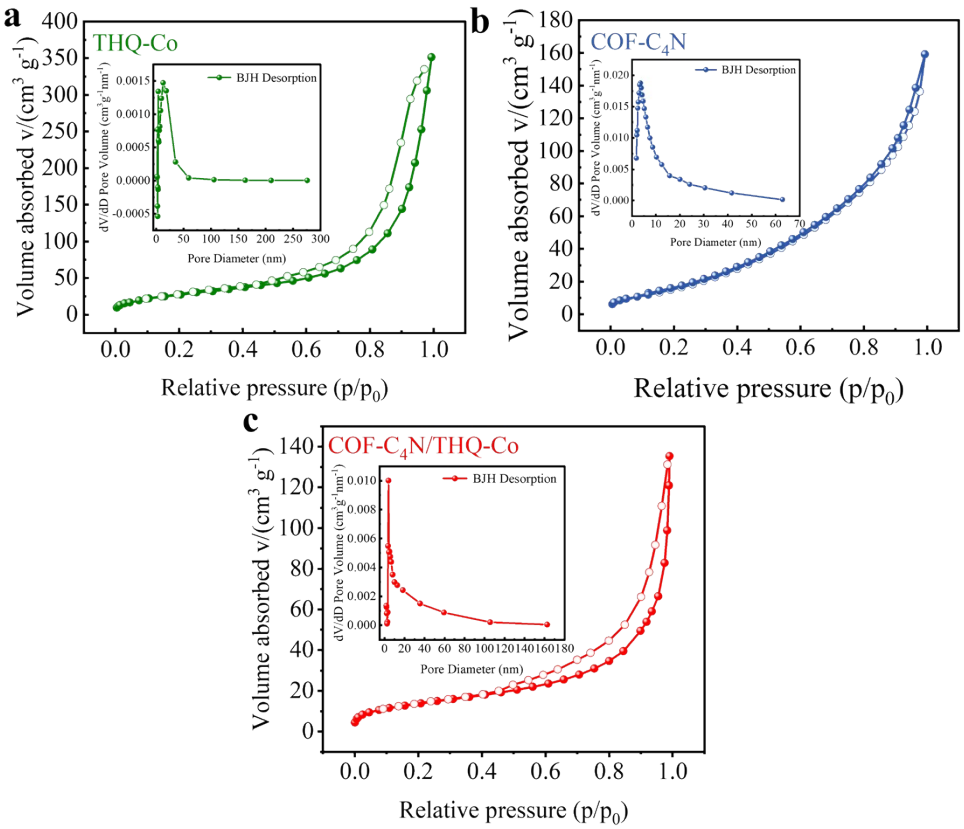

Fig. S11 N_2 adsorption isotherms and BJH desorption pore size distribution curves (inserted) for (a) THQ-Co, (b) COF-C_4N, and (c) COF-C_4N/THQ-Co.

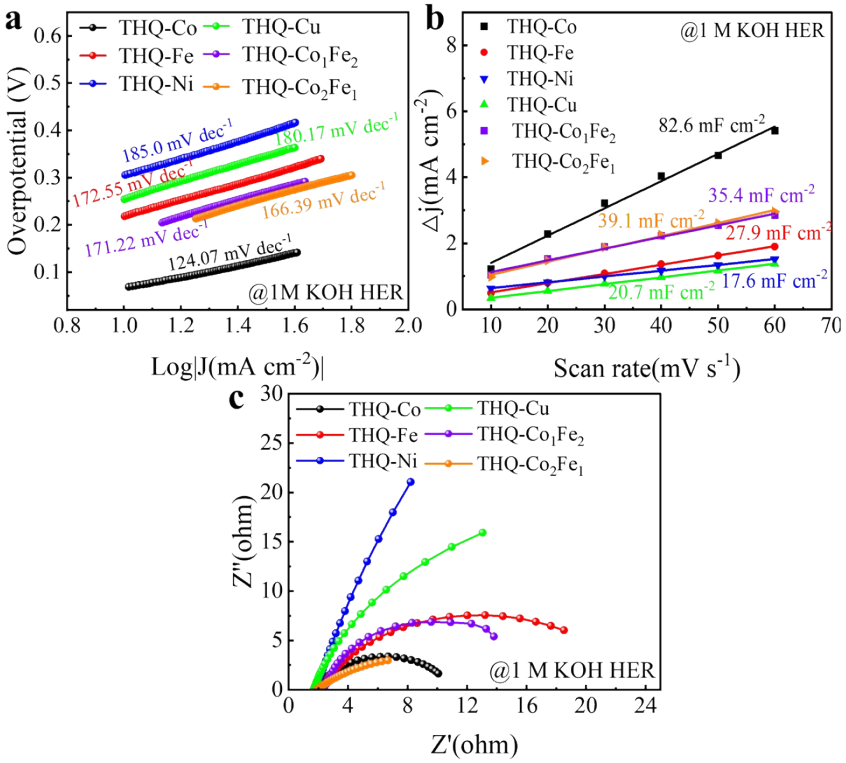

Fig. S12 (a) Tafel plots of alkaline HER with different metal THQ-M obtained after LSV treatment; (b) plots of capacitance currents versus scanning rates obtained based on CV curves; (c) Nyquist plot for THQ-M alkaline HER.

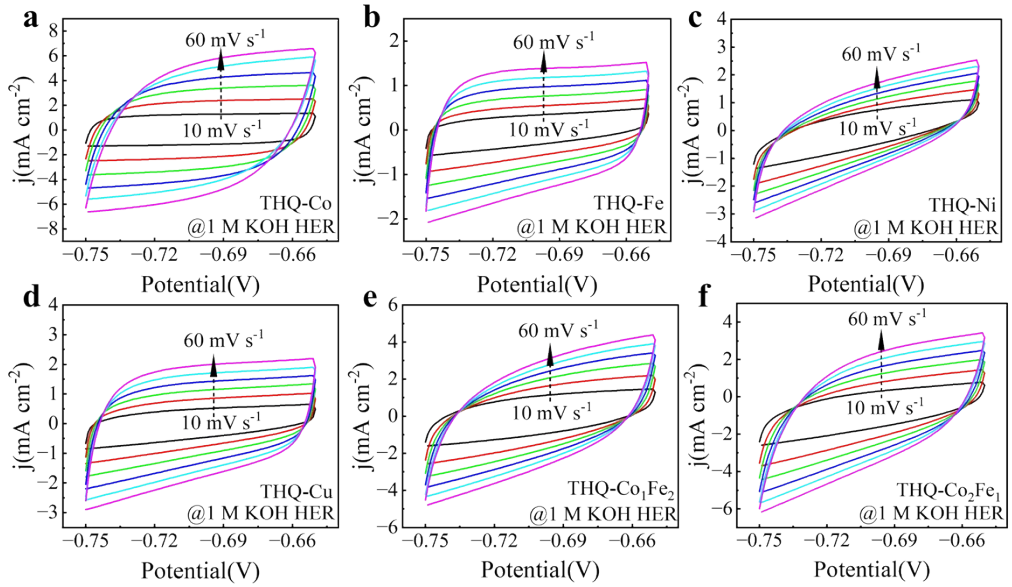

Fig. S13 (a-f) CV curves of THQ-M at different scanning speeds during the HER process.

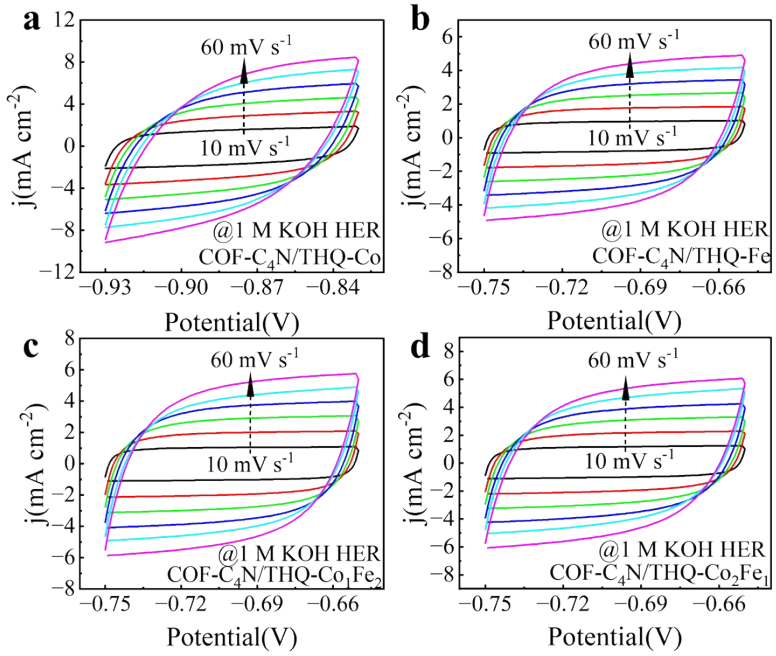

Fig. S14 CV curves of (a) COF-C_4N/THQ-Co, (b) COF-C_4N/THQ-Fe, (c) COF-C_4N/THQ-Co_1Fe_2, and (d) COF-C_4N/THQ-Co_2Fe_1 composite catalysts toward HER in alkaline media.

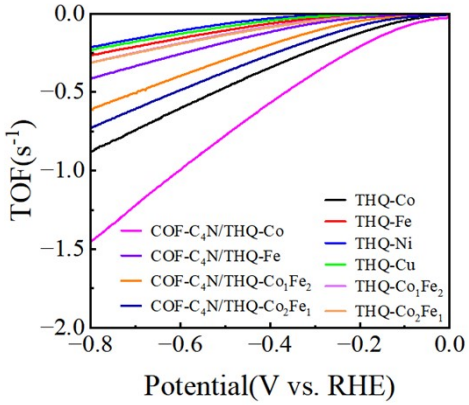

Fig. S15 Calculated TOF data for HER in alkaline media.

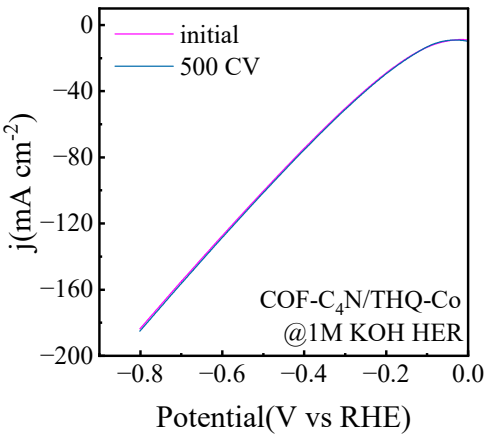

Fig. S16 LSV curves of COF-C_4N/THQ-Co before and after 500 cycles.

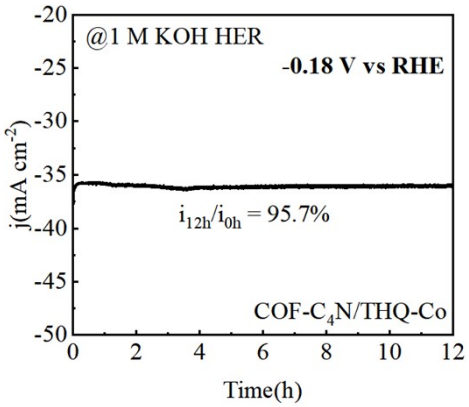

Fig. S17 The chronopotentiometric curves of COF-C_4N/THQ-Co at -0.18 V vs RHE for 12 h.

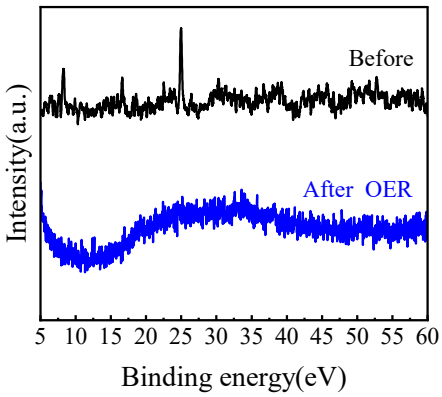

Fig. S18 XRD comparison of THQ-Co before and after electrocatalytic OER.

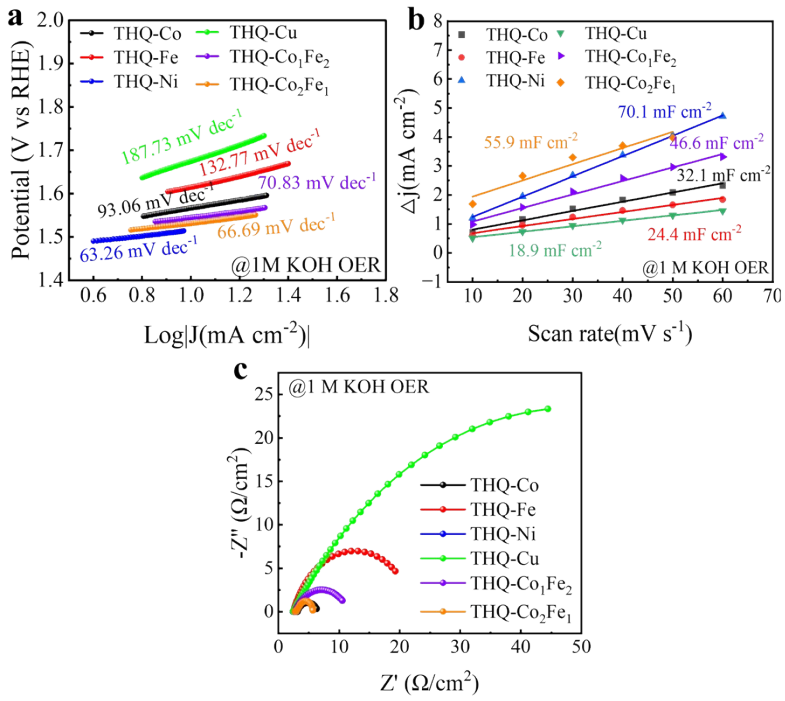

Fig. S19 (a) Tafel plots of alkaline OER with different metal THQ-M obtained after LSV treatment; (b) plots of capacitance currents versus scanning rates obtained based on CV curves; (c) Nyquist plot for THQ-M alkaline OER.

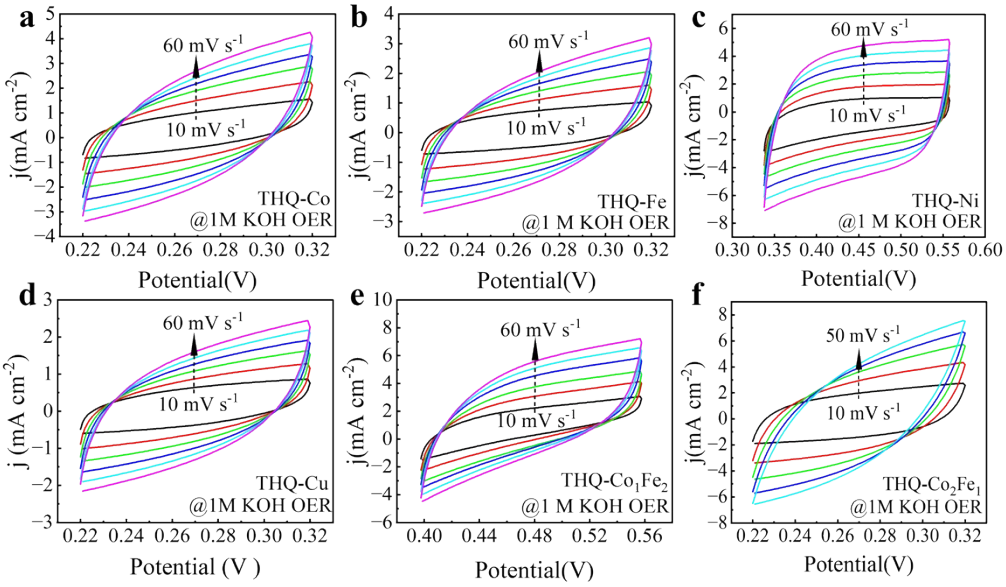

Fig. S20 (a-f) CV curves of THQ-M at different scanning speeds during the OER process.

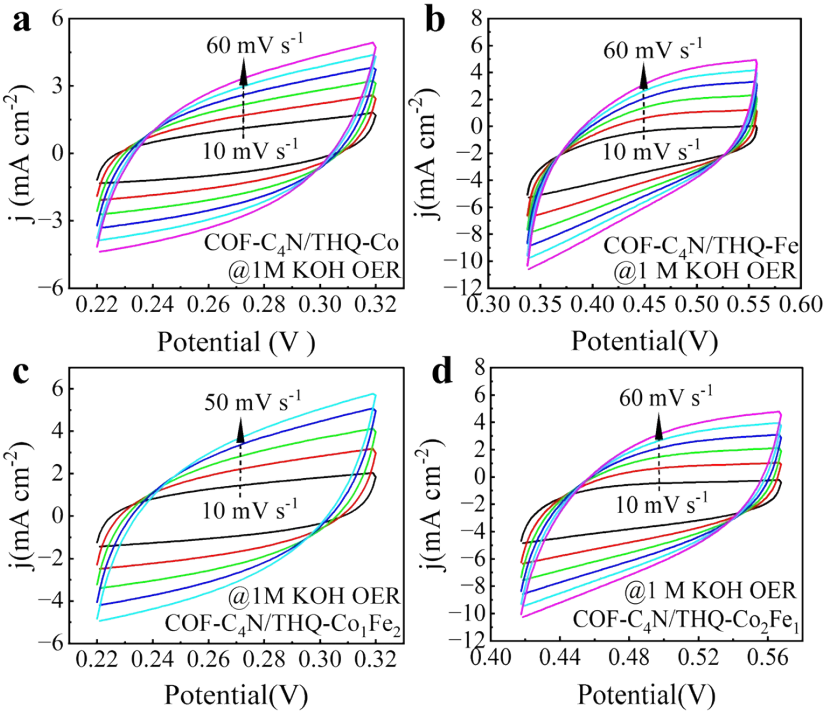

Fig. S21 (a-f) CV curves of COF-C_4N/THQ-M composite catalysts at different scanning speeds during the OER process.

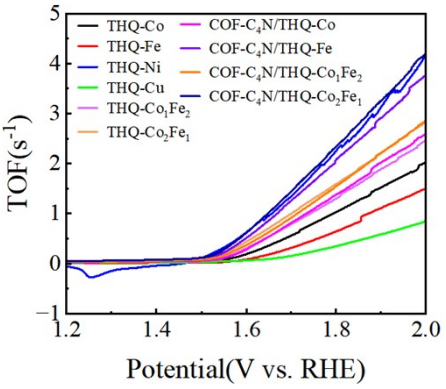

Fig. S22 Calculated TOF data toward OER in alkaline media.

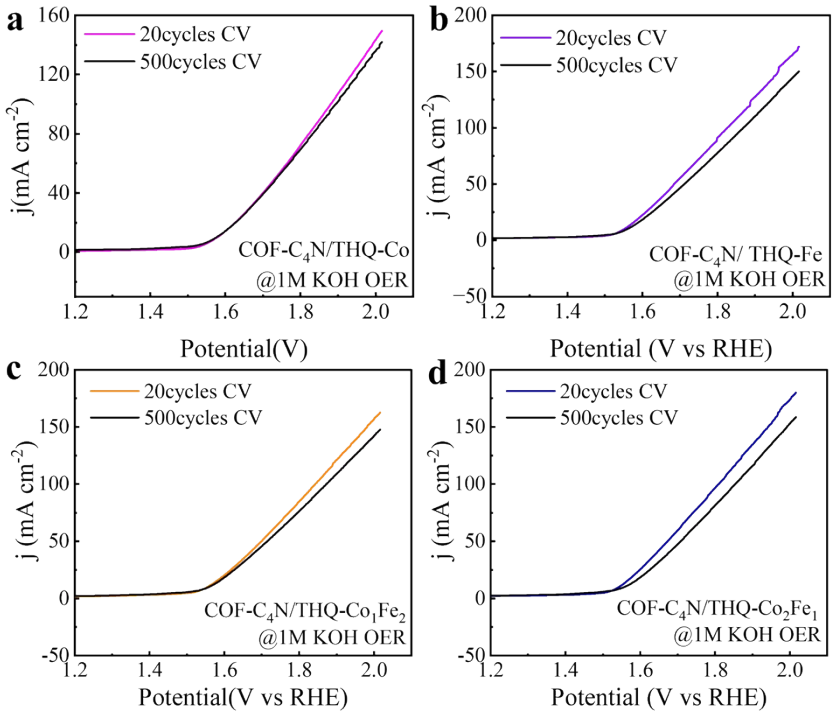

Fig. S23 LSV curves of COF-C_4N/THQ-Co before and after 500 cycles.

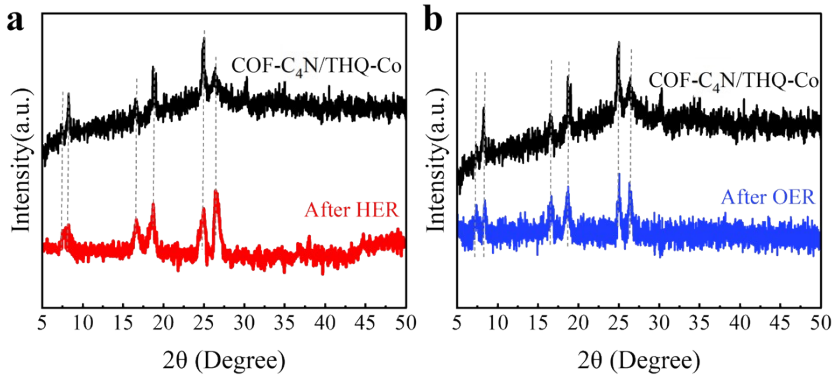

Fig. S24 XRD patterns of COF-C_4N/THQ-Co after stability tests for a) HER, b) OER in 1 M KOH media.

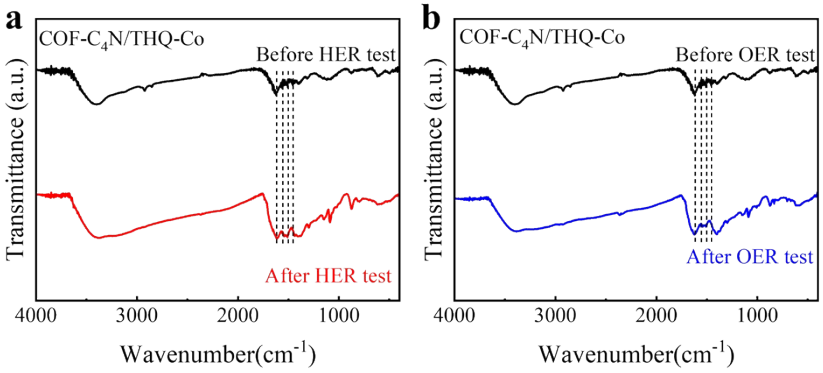

Fig. S25 The FT-IR spectra of COF-C_4N/THQ-Co before (black) , (a) after (red) the HER chronoamperometry test, and (b) after (blue) the OER chronoamperometry test.

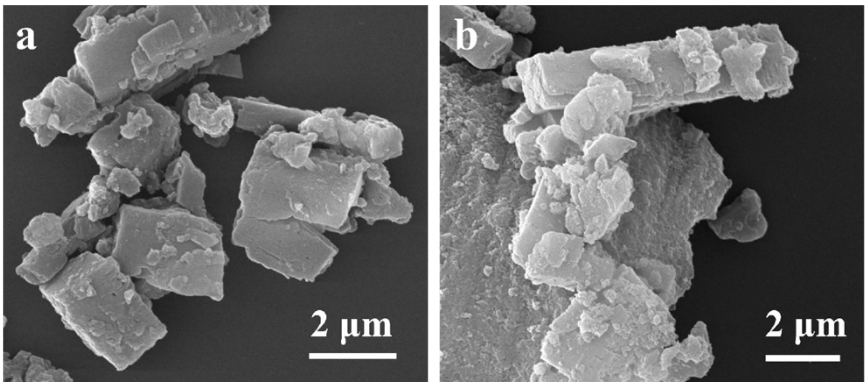

Fig. S26 The SEM images of COF-C_4N/THQ-Co, after (a) HER and (b) OER chronoamperometry test.

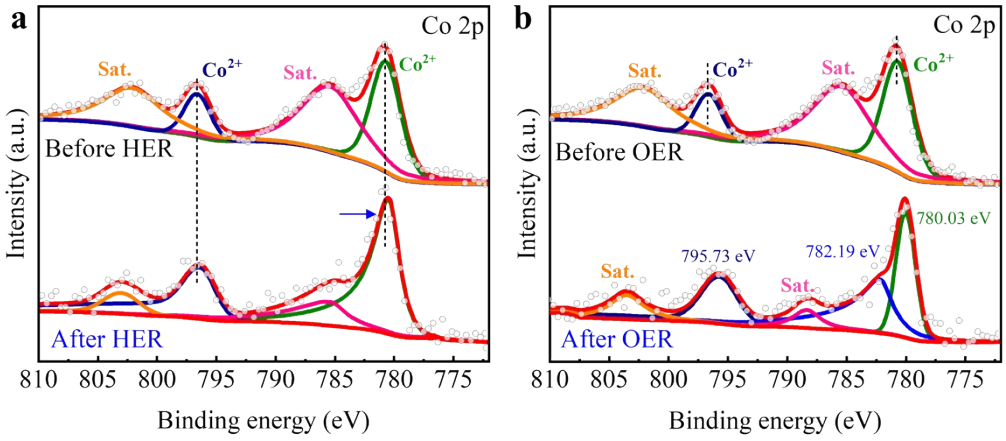

Fig. S27 The XPS Co 2p spectra of COF-C_4N/THQ-Co respectively after stability tests for (a) HER and (b) OER in 1.0 M KOH media.

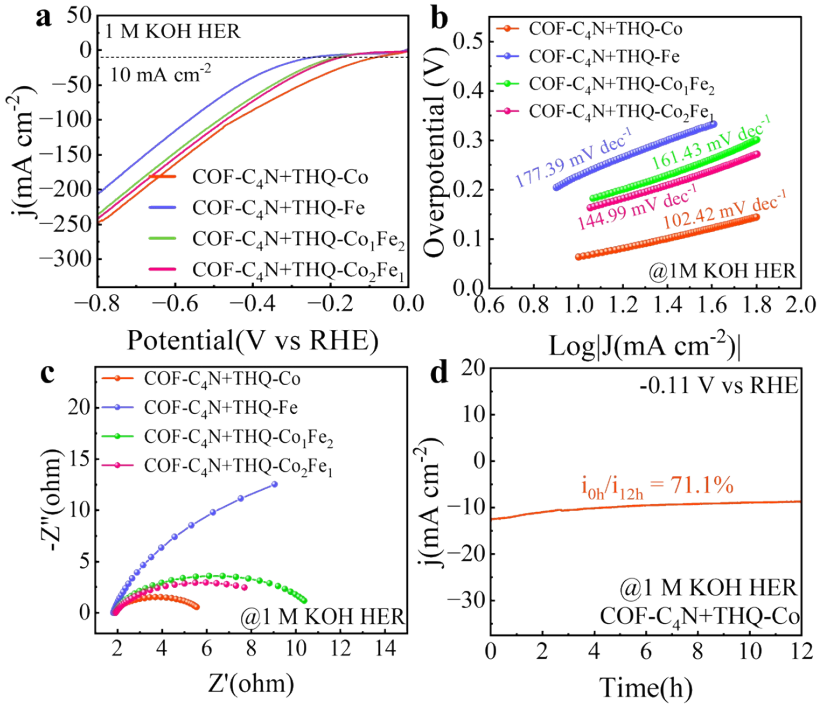

Fig. S28 (a) LSV curves, (b) Tafel slopes, and (c) EIS spectra of COF-C_4N+THQ-Co, COF-C_4N+THQ-Fe, COF-C_4N+THQ-Co_1Fe_2, COF-C_4N/THQ-Co_2Fe_1 toward HER in alkaline media, (d) chronopotentiometric curves of COF-C_4N+THQ-Co at -0.11 V vs RHE for 12 h.

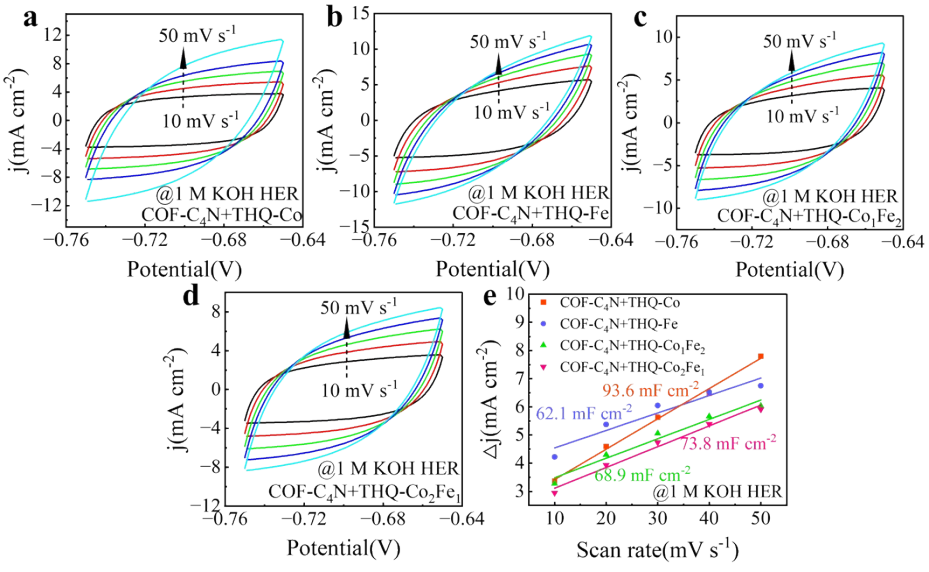

Fig. S29 CVs for (a) COF-C_4N+THQ-Co, (b) COF-C_4N+THQ-Fe, (c) COF-C_4N+THQ-Co_1Fe_2, (d) COF-C_4N/THQ-Co_2Fe_1 toward HER in alkaline media, (e) C_{dl} values.

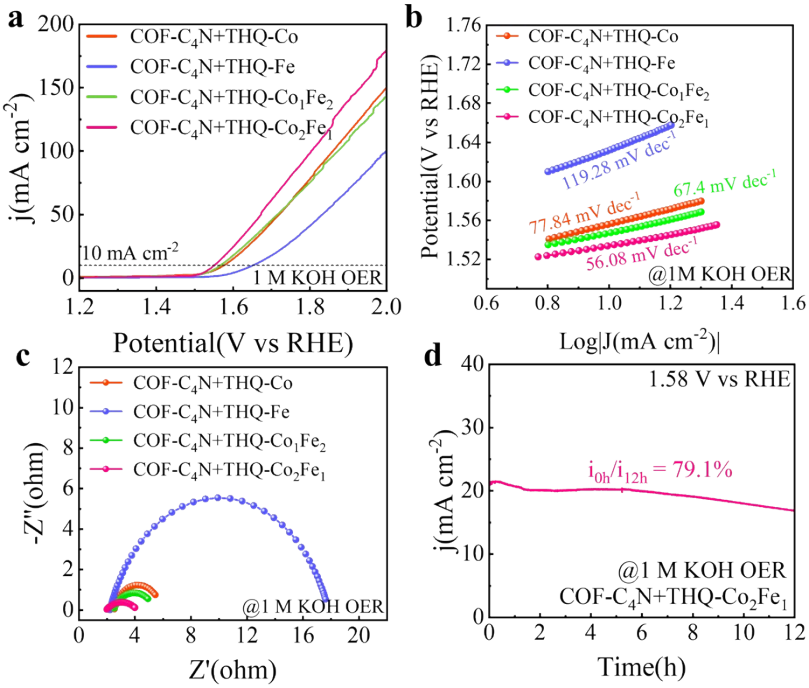

Fig. S30 (a) LSV curves, (b) Tafel slopes, and (c) EIS spectra of COF-C_4N+THQ-Co, COF-C_4N+THQ-Fe, COF-C_4N+THQ-Co_1Fe_2, COF-C_4N/THQ-Co_2Fe_1 toward OER in alkaline media, (d) chronopotentiometric curves of COF-C_4N+THQ-Co_2Fe_1 at 1.58 V vs RHE for 12 h.

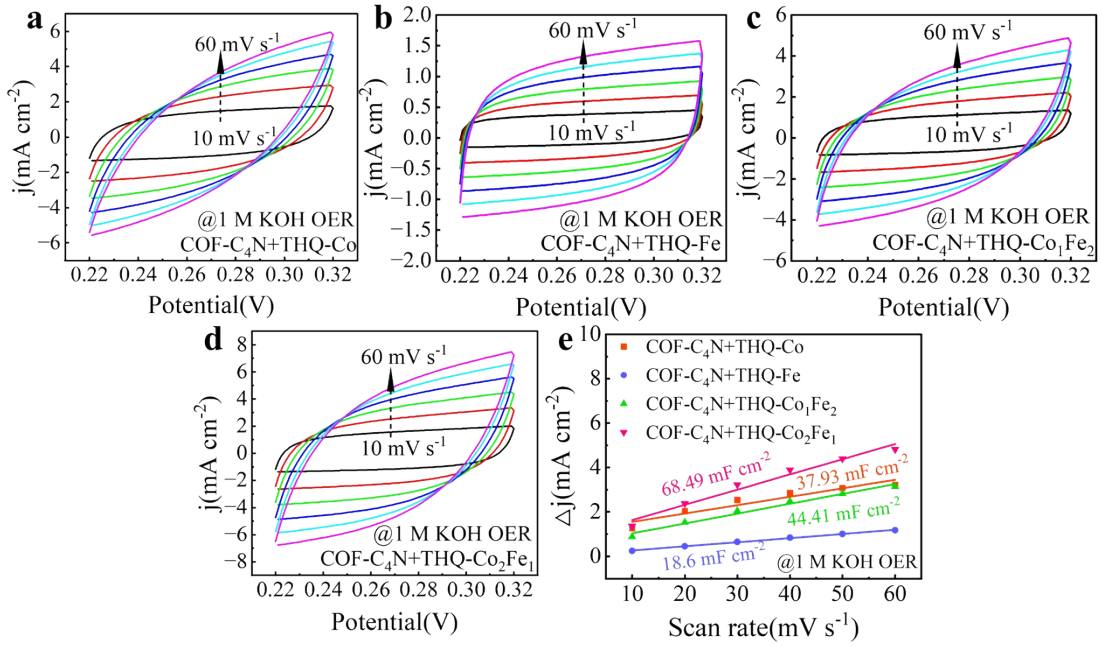

Fig. S31 CVs for (a) COF-C_4N+THQ-Co, (b) COF-C_4N+THQ-Fe, (c) COF-C_4N+ THQ-Co_1Fe_2, (d) COF-C_4N/THQ-Co_2Fe_1 toward OER in alkaline media, (e) C_{dl} values.

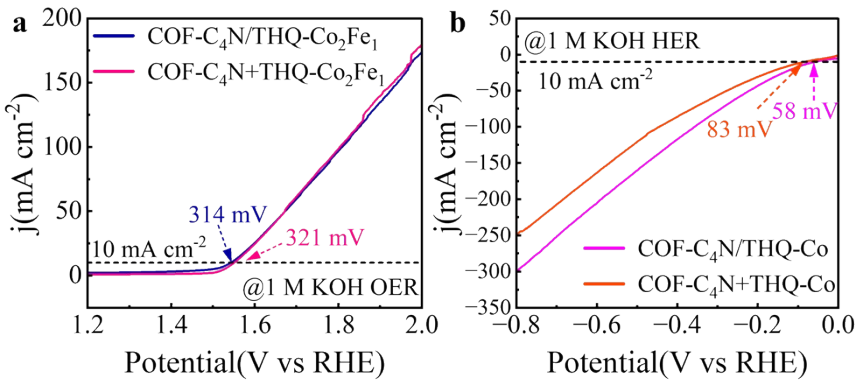

Fig. S32 (a) Comparison of OER polarization curves of COF-C_4N/THQ-Co_2Fe_1 and COF-C_4N+THQ-Co_2Fe_1 in alkaline media, (b) Comparison of HER polarization curves of COF-C_4N/THQ-Co and COF-C_4N+THQ-Co in alkaline media.

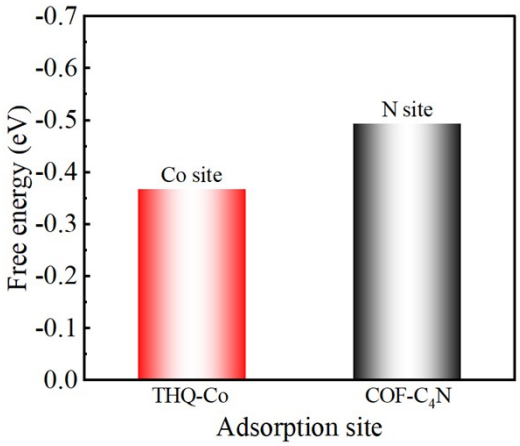

Fig. S33 The calculated ΔG_{H^*} of the THQ-Co and COF-C_4N catalyst at different hydrogen adsorption sites for HER.

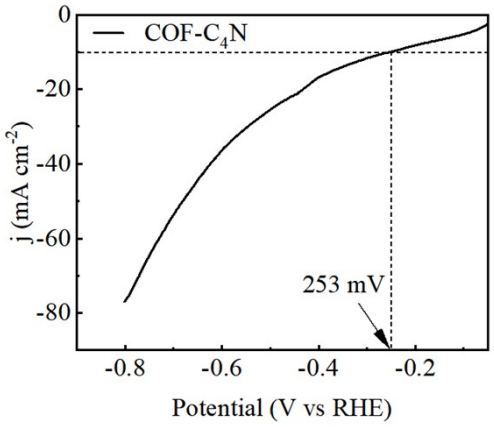

Fig. S34 HER polarization curves of COF-C_4N in alkaline media.

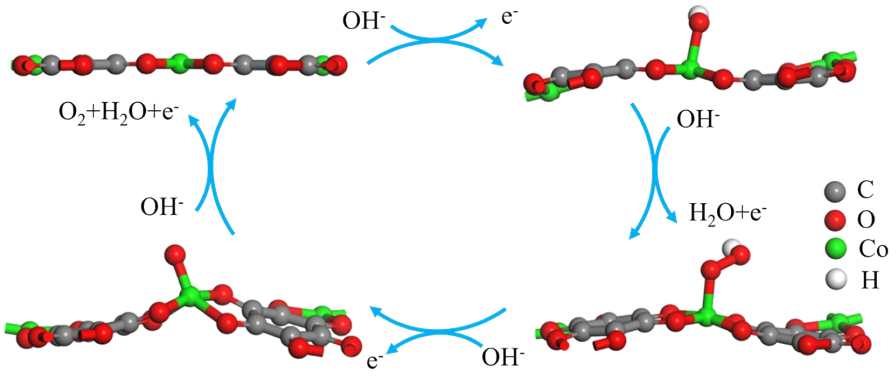

Fig. S35 Configurations of reaction intermediates on the reaction pathways of the oxygen evolution of THQ-Co. C: gray balls; O: red balls; Co: green balls; H: white balls.

Supplementary Table

Table S1. ICP-OES data of elemental Co content in THQ-Co and COF-C_4N/THQ-Co

Sample	Sample quality m_0 (g)	Test element	Test solution element concentration C_o (mg/L)	Sample element content C_X (mg / kg)	Sample element content w (%)
THQ-Co	1.64×10^{-2}	Co	8.89	270975.61	27.10%
COF-C_4N/THQ-Co	5.39×10^{-2}	Co	3.36	156009.22	15.60%

Table S2. Pore volume distribution of micro- and mesopores for THQ-Co, COF-C_4N, and COF-C_4N/THQ-Co

	micro porosity (%)	meso porosity (%)
THQ-Co	7.65	92.35
COF-C_4N	7.70	92.30
COF-C_4N/THQ-Co	9.33	90.67

Table S3. ICP-OES data of elemental Co content in COF-C_4N/THQ-Co after electrocatalytic OER and HER

	Sample quality m_0 (g)	Test element	Test solution element concentration C_o (mg/L)	Sample element content C_X (mg / kg)	Sample element content w (%)
HER	4.94×10^{-2}	Co	2.68	135429.87	13.54%
OER	4.87×10^{-2}	Co	2.28	116903.65	11.69%

Table S4. Comparison of electrocatalysts for HER under alkaline conditions

Catalyst	Electrolyte	η @-10 mA cm^{-2}（mV）	References
Co@NCNTs-800	1.0 M KOH	240	New J. Chem. 2017, 41, 10966-10971.
Co-1T-MoS_2-bpe	1.0 M KOH	118	Angew. Chem. Int. Ed. 2023, 62, e202313845.
MoCx	1.0 M KOH	151	Nat. Commun. 2015, 6, 6512.
CoPS/N-C	1.0 M KOH	148	Nanoscale 2018, 10, 7291-7297.
Fe-Ni@NC-CNTs	1.0 M KOH	202	J. Alloys Compd. 2021, 850, 156583.
FeCoNi MOF/NF	1.0 M KOH	116	J. Am. Chem. Soc. 2022, 144, 3411-3428.
$Fe(OH)_x$@Cu-MOF	1.0 M KOH	112	Sci. Adv. 2021, 7, eabg2580.
D-Ni-MOF NSA	1.0 M KOH	101	Small 2020, 16, 1906564.
RuO_2/Co_3O_4	1.0 M KOH	89	RSC Adv. 2017, 7, 3686-3694.
MoS_2/NiCo-LDH	1.0 M KOH	78	Joule 2017, 1, 383-393.
FeS/FeOOH-ZnO@NF	1.0 M KOH	74	K. Alloys Compd. 2024, 991, 174525.
CuCo-CAT/CC	1.0 M KOH	52	Adv. Mater. 2021, 33, 2106781.
COF-C_4N/THQ-Co	1.0 M KOH	58	This work
COF-C_4N/THQ-Co_2Fe_1	1.0 M KOH	132	This work

Table S5. Comparison of electrocatalysts for OER under alkaline conditions

Catalyst	Electrolyte	η @10 mA cm^{-2}（mV）	References
Co_3ZnC/Co	1.0 M KOH	366	J. Mater. Chem. A 2016, 4, 9204-9212.
NNU-23	0.1 M KOH	365	Angew. Chem. Int. Ed. 2018, 57, 9660-9664.
COF@CNT	1.0 M KOH	350	Chem. Eng. J. 2021, 415, 127850.
COF-C_4N	1.0 M KOH	349	ACS Energy Lett. 2019, 4, 2251-2258.
N-MoS_2/COF-C_4N	1.0 M KOH	349	SSRN 2023, 13, 90-101.
Ni-COF	1.0 M KOH	335	JACS Au 2021, 1, 1497-1505.
Co-COF@MOF	1.0 M KOH	328	Small 2024,20,2308598.
Fe-Co_2P@NPDC	0.1 M KOH	320	Chem. Eng. J. 2022, 446, 137210.
$Ni_{0.5}Fe_{0.5}$@COF-SO_3	1.0 M KOH	308	Inorg. Chem. 2020, 59, 4995-5003.
Co_3Fe-MOF	1.0 M KOH	280	J. Mater. Chem. A 2020, 8, 3658-3666.
USTA-16	1.0 M KOH	408	Mater. Interfaces 2017, 9, 7193.
CoO_x-ZIF	1.0 M KOH	318	Adv. Funct. Mater. 2017, 27, 1702546.
FeNi@NC	1.0 M NaOH	280	Environ. Sci. 2016, 9, 123
FeCo@CNTs-60	0.1 M KOH	440	Appl. Catal. B Environ. 2024, 341, 123346
COF-C_4N/THQ-Co_2Fe_1	1.0 M KOH	314	This work

COF-C_4N/THQ-Co	1.0 M KOH	339	This work